Soft Matter

Accepted Manuscript

ROYAL SOCIETY OF CHEMISTRY

www.rsc.org/softmatter

(Soft Matter)

Synthesis of Crosslinked Polymeric Nanocapsules using Catanionic Vesicle Templates Stabilized by Compressed CO_2

Siming Dong, Patrick T. Spicer, Frank P. Lucien, Per B. Zetterlund*

Centre for Advanced Macromolecular Design (CAMD), School of Chemical Engineering, The University of New South Wales, Sydney, NSW 2052, Australia
Tel: +61 2 9385 4331; Fax:+61 2 9385 6250; E-mail: p.zetterlund@unsw.edu.au

* Corresponding author

Abstract: The synthesis of polymeric nanocapsules in the approximate diameter range 40-100 nm (TEM/SEM) using catanionic surfactant vesicle templates stabilized by subcritical CO_2 is demonstrated. Near equimolar aqueous solutions of the surfactants sodium dodecyl sulfate (SDS) and dodecyltrimethylammonium bromide (DTAB) experienced immediate vesicle destabilization and precipitation in the absence of CO_2. However, pressurization with CO_2 (5 MPa) dramatically enhanced the stability of the initial vesicles, and enabled swelling of the bilayers with hydrophobic monomers via diffusion loading (loading of monomers into preformed bilayers). Subsequent radical crosslinking polymerization of the monomers *n*-butyl methacrylate/*tert*-butyl methacrylate/ethylene glycol dimethacrylate contained within the bilayers was conducted at room temperature using UV-initiation under CO_2 pressure. The hollow structure of the resultant nano-objects was confirmed by successful encapsulation and retention of the dye Nile Blue. It is demonstrated that using this method, polymeric nanocapsules can be successfully prepared using diffusion loading of up to 94 wt% monomer (rel. to surfactant) stabilized by CO_2.

Introduction

Polymeric nano-objects of different shapes/morphologies can be prepared by a variety of means using for example emulsion-based approaches,[1-3] self-assembly based techniques,[4-6] as well as methods based on templating.[7, 8] Hollow polymeric nanoparticles (nanocapsules)[9-12] are interesting as they offer the potential of various applications such as coatings, cosmetic applications, and drug delivery, whereby a drug can be contained by the interior of the capsule and the release rate controlled by the nature of the shell.[13-15] There are a number of ways to synthesize polymeric nanocapsules, such as phase separation within polymer particles during polymerization in aqueous dispersed systems,[16-19] various techniques involving removal of sacrificial core material from core-shell particles where the shell is polymeric,[20-22] as well as miniemulsion templating.[7, 23]

A unilameller vesicle is a colloidal structure, usually spherical, comprising amphiphilic species in a single bilayer that encloses an aqueous interior volume.[24] In Nature, such bilayers are found in cell membranes, the main component being phospholipids. Vesicles exhibit great structural versatility and as such find a wide range of applications in for cell mimetic systems, drug and gene delivery, cosmetics, food science, and nanoreactor chemistry.[25-29] Unilamellar vesicles are usually prepared by swelling phospholipid films in excess water to make multilamellar vesicles, followed by mechanical disruption, such as sonication or extrusion through filters. This complex technique involves the use of toxic solvents (such as chloroform) as well as the use of high-energy devices. Kaler et al. reported[30, 31] that catanionic vesicles[25, 32] can form spontaneously in aqueous mixtures of cationic and anionic single chain surfactants. Mixtures of cationic and anionic surfactants can result

in spontaneous formation of vesicles as a result of the generation of complexes of surfactants of opposite charge. This arrangement causes a decrease in the average area of the surfactant head group, and consequently an increase in the value of the packing parameter[33] – this explains why the individual surfactants tend to form spherical micelles, yet vesicles are formed in the corresponding mixed surfactant system.[34] These spontaneous vesicular systems have attracted attention due to their simplicity and low-energy requirement in contrast to vesicles formed from lipids and other double-chained surfactants. However, the method has its limitations due to its sensitivity. In many cases, cationic and anionic surfactants tend to precipitate due to strong ion pairing and partial shielding of charges. For example, sodium dodecylbenzenesulfonate (SDBS) and cetyltrimethylammonium tosylate (CTAT) can form stable vesicles only when one of the surfactants is present in great excess.[30]

The use of vesicles as polymerization templates for polymeric nanocapsule synthesis relies on swelling of the bilayers with monomer,[35] which is subsequently polymerized.[11, 36-44] Ideally, this enables one to create a polymer nanocapsule of the same shape as the original vesicle, although there are sometimes issues related to vesicle stability and phase separation leading to more complex morphology.[45] Vesicle-templated polymeric nanocapsules can provide additional benefits such as the control of permeability, fast diffusion of ions and long-term stability in contrast to other hollow polymer particles.[46-49] Attractive features of the vesicle template approach also include the ability to synthesize very small nanocapsules (diameter < 100 nm) as well as good control over the nanocapsule structural design. Kaler and coworkers[44] reported polymerization in bilayers of surfactant vesicles using 10 wt% monomer (rel. to surfactant weight), obtaining hollow polymer particles with a diameter of 60 nm. However, it was also reported by other groups that solid latex particles with "parachute" structure can be obtained due to poor vesicle stability and phase separation during the polymerization.[43, 45, 50, 51] Recently, Pinkhassik and coworkers developed a concurrent monomer loading method whereby surfactants and monomer are added simultaneously to water (as opposed to diffusional loading, which entails swelling of the bilayer by adding monomer to pre-formed vesicles) for the synthesis of vesicle-templated polymer nanocapsules.[52-54]

It is well-established that subcritical CO_2 can be used as a stimulus in changing the properties of surfactant aggregates in aqueous solutions.[55] It was reported in 2009 that catanionic vesicle stability can be dramatically enhanced by use of subcritical CO_2 (< 7 MPa).[56] It has been proposed that the non-polar CO_2 molecules can insert into the bilayer region of the vesicles to reduce the size of the vesicles and increase the rigidity of the membrane, and therefore enhance the vesicle stability.[56] Similar results have been obtained using other compressed gases, *e.g.* methane, ethane and ethylene.[57] Vesicles that would normally degrade more or less instantaneously can be stabilized via pressurization to have lifetimes of the order of hours, thus enabling their use as

nanoreactors or polymerization templates. Moreover, subcritical CO_2 can be effectively used to control the vesicle size,[56] as well as to effect micelle-to-vesicle transitions reversibly.[58] This green technique, relying on environmentally friendly and inexpensive CO_2, has the potential to greatly increase the scope and versatility of the various applications of vesicles.

In the present paper, the preparation of polymeric nanocapsules using catanionic surfactant vesicle templates stabilized by compressed CO_2 is presented. It is shown that spontaneous catanionic vesicles formed by self-assembly of surfactant mixtures with hydrophobic monomer building blocks can be effectively stabilized by subcritical CO_2. Polymeric nanocapsules are obtained by UV-initiated radical crosslinking polymerization under CO_2 pressure, followed by the removal of surfactants.

Experimental section

Materials. *n*-Butyl methacrylate (*n*-BMA; Aldrich, 99%), *tert*-butyl methacrylate (*t*-BMA; Aldrich, 98%) and ethylene glycol dimethacrylate (EGDMA; Aldrich, 98%) were purified by passing through a column of basic aluminum oxide (Ajax) before use. Sodium dodecyl sulfate (SDS; Aldrich, 99%), dodecyltrimethylammonium bromide (DTAB; Aldrich, 98%), Nile Blue A (NBA, Aldrich), potassium persulphate (KPS, Aldrich, 99.9%), phenylbis(2,4,6-trimethylbenzoyl)phosphine oxide (Irgacure 819, Aldrich, 97%), and liquid CO_2 (Coregas, 99.5%) were used as received. Distilled and deionized (DI) water was used in the experiments.

Vesicle stability before polymerization. Phase behavior observations were conducted in a modified Jerguson sight gauge reactor with an internal volume of 40 mL. A detailed description of the reactor setup is given elsewhere.[59] Monomers and initiator (*n*-BMA (1.0 g (7.0 mmol)), *t*-BMA (1.0 g (7.0 mmol)), EGDMA (1.0 g (5.0 mmol)) and Irgacure 819 (0.10 g (0.239 mmol))) were mixed to make up a monomer stock solution. In a typical experiment (Table 1), SDS and DTAB were separately dissolved in DI water in two Cospak bottles with magnetic stirring for 20 min at ~40 °C. The temperature of the empty reactor was set to 36 °C. Both surfactant solutions were then weighed and transferred into the reactor followed by gentle magnetic stirring (100 rpm) for a very short time (< 10 s). The monomer stock solution (40 μL) was subsequently added to the reactor using a micropipette in the absence of stirring such that an upper monomer layer formed (stirring at this stage caused precipitation). The reactor was sealed and stirring initiated after the mixture was added. The reactor was immediately covered with aluminum foil and purged with low pressure CO_2 (0.5 MPa) to remove oxygen. CO_2 was added to the reactor to the desired pressure (5.0 MPa in most experiments). The system was then allowed to stabilize for 15 min with magnetic stirring (300 rpm).

The temperature was subsequently reduced to 25 °C. After thermal equilibrium had been established (~10-15 min), additional CO_2 was added to the reactor to compensate for the pressure loss caused by the decrease in temperature. Phase behavior was observed through the sight gauge.

Synthesis of nanocapsules. The reactor used for phase behavior observation was also used for polymerizations. In a typical experiment, the vesicle solution was prepared as described above. The solution was kept under stirring (300 rpm) overnight at 25 °C under CO_2 pressure to allow the monomer to diffuse into the vesicle bilayers. The monomer-loaded vesicle solution was then irradiated for 2 h with UV light (λ = 390 nm) via the glass windows of the reactor using two LED lamps (~15 W, Shenzhen Guyou Special Light Source), one on either side of reactor; the distance between the lamps and the reactor was 4 cm on both sides. After the polymerization, the reactor was depressurized slowly over ~30 min. The resulting nanocapsules were precipitated in methanol. The liquid was decanted, and the precipitate was washed three times with methanol and water to remove surfactants and unreacted monomers.

Dye retention experiment. An aqueous solution of the dye Nile Blue A (NBA) was used for the preparation of surfactant solution instead of pure water. The nanocapsules were prepared as per the steps described above. The resulting nanocapsules were precipitated in methanol. The liquid was decanted, and the precipitate was washed five times with methanol:water (1:1 vol:vol) to remove surfactants, unreacted monomers and non-encapsulated free dye.

Measurements and characterization. The surface morphology and shape of the nanocapsules were observed using a field-emission scanning electron microscope (Nova NanoSEM 230, FEI, USA) at an accelerating voltage of 3 kV – 5 kV with a spot size of 2.5 µm. Each sample was sputter coated with chromium for 20 s at 20 mA (Emitech K575X Peltier Cooled Sputter Coater; Emitech Products Inc., USA). The size and morphology of nanocapsules were observed using a transmission electron microscopy JEOL1400 TEM at an accelerating voltage of 100 kV. The suspension was directly taken and diluted with water. One drop of diluted sample was deposited onto a copper grid (ProSciTech). 2% Phosphotungstic acid solution as negative staining was applied for all samples. Online dynamic light scattering (DLS) measurements were performed *in situ* under CO_2 pressure using a specifically designed Cordouan Particle Size Analyzer with a 75 mW laser source operating at 658 nm in backscattering light detection mode. The backscattered light was recorded at 135° by an APD detector. The data were analyzed using NanoQ software. All DLS data in this work was acquired under CO_2 pressure.

Results and Discussion

Vesicle stability before polymerization. As outlined in the Introduction, when aqueous solutions of SDS and DTAB are mixed, vesicles are formed spontaneously. However, when the stoichiometry is in the vicinity of 1:1 (molar ratio), such mixtures tend to form a lamellar structure or precipitate due to formation of the equimolar precipitate DTA^+DS^-.[30, 60] The highly symmetric linear-chained DTAB/SDS pairs can pack into a crystalline lattice, resulting in the formation of precipitate and vesicle degradation.[60] Previous work has demonstrated that the rate of such vesicle degradation can be reduced by pressurization with CO_2.[56] For DTAB/SDS, the system remained stable for five days or more for CO_2 pressures above 4 MPa. Using these results as a guide, 5.0 MPa was used in the present work.

In order to use catanionic vesicles as templates for radical polymerization within the bilayer, it is important to investigate the stability of such catanionic vesicle solutions in the presence of vinyl monomer (*i.e.* swelling of bilayer with monomer as described in the experimental section; *n*-BMA, *t*-BMA, EGDMA) with and without CO_2 pressurization. In order to slow down the rate of precipitate formation before CO_2 pressurization, the temperature was set to 36 °C, *i.e.* above the Krafft point of DTA^+DS^- of 35 °C.[61] The temperature was subsequently decreased to 25 °C after CO_2 pressurization. Successful so called concurrent monomer loading (*i.e.* water, surfactants and monomer are mixed in one single step) of catanionic vesicles has been reported.[52-54] However, in the present work, this approach led to precipitation due to the molar ratio of surfactants being close to 1:1. The approach of diffusional loading adopted in the present study entailed careful addition of the monomer to the aqueous surfactant solution such that an upper monomer layer initially formed, after which CO_2 was introduced and stirring commenced. It thus appears that the presence of monomer has a destabilizing effect on the vesicles under these conditions.

Fig. 1 shows photographs of the solutions at different times with (5.0 MPa) and without CO_2 at 25 °C. In the absence of CO_2, the initially clear solution became markedly less transparent after a few minutes with a white crystalline precipitate forming. However, in the presence of CO_2, the solution remained transparent for several hours and became gradually less transparent after 24h, remaining slightly translucent after 33h, consistent with stabilization by CO_2. It thus appears that the stabilizing effect of CO_2 is operative also when the bilayer is swollen with monomer (47 wt% rel. to total surfactant).

The template synthesis of nanocapsules consists of three consecutive steps: (*i*) spontaneous formation of catanionic vesicles; (*ii*) diffusional loading of monomers; (*iii*) polymerization. In the second step, monomers are absorbed into the interior of the bilayer over time. After addition of

monomer to the aqueous surfactant mixture followed by CO_2 pressurization, the vesicle size was monitored as a function of time in the absence of polymerization using online DLS under CO_2 pressure (Fig. 1). The intensity-average diameters increased with time from ~120 nm to ~185 nm, consistent with the observed turbidity increase with time (Fig. 2). It should be noted that pressurization with CO_2 may influence the accuracy of the DLS results via alteration of the refractive index of the particles. DLS measurements on aqueous emulsions of polystyrene particles indicate that any effect CO_2 on the refractive index and/or viscosity of the continuous aqueous phase on the DLS results is negligible.[62] Fig. 3 shows the corresponding size distributions, revealing that a bimodal distribution developed after ~22h. It has been reported that for liposome vesicles, monomer can be fully loaded into bilayers in ~15h,[35] while for catanionic vesicles, the loading capacity can be reached in ~4h.[53] The size of the vesicles will increase slightly during this process.[35] In addition to the effect of monomer loading, after the initial formation of catanionic vesicles (in absence of monomer; the initial size typically depends on method of preparation[31]) their size tends to change with time due to equilibration. For example, in the case of SDBS/CTAT (cetyltrimethylammonium tosylate) it has been reported that it takes ~1 week for the equilibrium size to be reached.[31] In the present case, the observed size/distribution change of the vesicles before polymerization is probably a combined effect of the monomer-loading process and self-equilibrium of the vesicles. One can speculate that the smaller nano-objects (~20 nm) may be monomer-swollen spherical micelles, similar to what was previously observed by Dergunov et al.[52] for catanionic vesicles (not using CO_2). Bimodal size distributions after catanionic vesicle-templated polymerization (using concurrent loading without CO_2) have also been observed by Kim et al.,[54] who also showed that less bimodal character was achieved by extrusion prior to polymerization.

Vesicle-templated polymerization. Polymeric nanocapsules were synthesized by UV-initiated vesicle-templated crosslinking polymerization of *n*-BMA/*t*-BMA/EGDMA using Irgacure 819 (Scheme S1) as photoinitiator at 25 °C in the CO_2-pressurized reactor after overnight equilibration (the reactor was kept at 25 °C at a CO_2 pressure of 5.0 MPa for ~14 h prior to UV-initiation). After polymerization, the CO_2 was released over ~30 min, resulting in immediate formation of a white crystalline precipitate. The overall monomer conversion was in excess of 75% as determined by gravimetry. Fig. 4 shows TEM and SEM images of the polymerization product after purification, revealing spherical objects of diameters in the approximate range 40-100 nm, within the range of previously reported sizes of SDS/DTAB unilamellar vesicles.[63] The spherical shape of the nanocapsules was retained after repeated centrifugation and redispersion due to a sufficiently high degree of crosslinking. In addition, poly(*t*-BMA) has a relatively high glass transition temperature (~107 °C), thus providing good rigidity of the nanocapsules at room temperature. Polymerization

using the same recipe and identical conditions but in the absence of the crosslinker was also performed as a control experiment. In this case, however, only gel-like polymer aggregates were obtained after surfactant removal (by precipitation or dialysis against methanol and water). Similarly, Kim et al. also reported that catanionic vesicle-templated polymerization of butyl methacrylate in the absence of crosslinker did not result in formation of hollow particles.[52, 54]

A dye retention test was conducted to confirm the hollow structure of the particles following a previously reported approach[47] (Fig. S1). Nile Blue A (NBA) was added to the aqueous phase during the preparation of the vesicle solutions, followed by polymerization using the same procedure as above. The solution remained blue despite multiple washings with methanol (Fig. S1), indicative of NBA being retained within the nanocapsules, consistent with hollow structures. The presence of pores/pinhole defects in the polymeric shells may lead to the dye diffusing out of the core.[54] Given that the smallest cross-section of NBA is 1 nm,[52] it thus appears that there are no significant pores/pinholes in these capsules.

Effect of monomer loading. To investigate the effect of monomer content on vesicle solutions stabilized by CO_2, different monomer contents (70, 94 and 118 wt% rel. to total surfactant, to be compared with 47 wt% above) were used in the preparation and polymerization of the monomer-loaded vesicles. Online DLS was used to measure the particle size before and after polymerization under CO_2 pressure. For 70 and 94 wt% monomer, the size distributions after stirring under CO_2 pressure of 5.0 MPa (before polymerization) revealed an increase in size and development of a bimodal distribution between 12 and 18h, similar to the case of 47 wt% monomer (Fig. 3). There was no significant change in size and size distribution before and after polymerization (Fig. 5A and 5B). However, using the highest monomer loading of 118 wt%, a clear oil layer was observed initially at the top of the solution. The oil layer disappeared after 4h stirring (before polymerization but under 5.0 MPa CO_2 pressure), the vesicle solution became more turbid (Fig. S2), which probably indicates that the maximum capacity of monomer loading had been reached[64] or possibly lower vesicle stability at high monomer loading. At this point, the DLS size distribution was similar to those of 70 and 94 wt% monomer loading. However, upon polymerization, a shift to larger objects was observed (Fig. 5C). The intensity-average diameters corresponding to the three monomer loadings discussed above are listed in Table 2, revealing similar sizes before/after polymerization for 70 and 94 wt%, and a more significant increase for 118 wt% monomer.

The morphology of the obtained nanocapsules after surfactant removal at different monomer loadings was observed using TEM and SEM (Fig. 6). For 70-94 wt% (Fig. 6 A-D), the size and shape of the nanocapsules were similar to the nanocapsules prepared using lower monomer content. However, for 118 wt% (Fig. 6 E, F), a small number of large particles with a diameter >1 μm was

observed by SEM (not observed for lower monomer contents). These large particles can probably be attributed to excess monomer being present as monomer droplets and subsequently undergoing polymerization via monomer droplet nucleation. Since the number of such droplets is not substantial, they were not detected by DLS.

To date, two types of loading methods have been reported for the preparation of monomer-loaded vesicle solutions; diffusion loading (loading of monomers into preformed bilayers) and concurrent loading (loading of monomers during the formation of bilayers).[30, 40, 43, 44, 50, 52-54] However, the addition of monomer can be disruptive to the formation of vesicles according to the process of diffusion loading.[43, 44] Therefore, when vesicles are used as templates in this manner, the monomer content has typically only been 10-20 wt% using diffusion loading. In the present work, it has been shown that nanocapsules can be successfully prepared using diffusion loading up to 94 wt% monomer relative to surfactant, which is comparable to the higher levels of monomer loading typically achievable with concurrent loading.[52-54]

Effect of CO_2 pressure. The synthesis of nanocapsules was also performed at 3.5 MPa (as opposed to 5.0 MPa above) to evaluate the effect of CO_2 pressure. As shown in Fig. S3, the solution became turbid ~1h after the addition of monomer (47 wt% rel. to total surfactant), more rapidly than all other cases at 5.0 MPa. DLS data revealed no large aggregates before or after polymerization at 3.5 MPa (Fig. S3B). However, SEM (Fig. 7) analyses revealed the presence of objects in the micron-scale (1-2 μm), although the small objects were similar in size to the nanocapsules prepared at 5.0 MPa. The turbidity observed after 1h may thus be related to (*i*) the presence of large vesicles as observed previously[56] and/or monomer droplets as discussed above, suggesting insufficient vesicle stability at this lower CO_2 pressure. There appears to be no significant relationship between the CO_2 pressure and the size of nanocapsules (the population of submicron-size particles) in this particular case, despite a previous report demonstrating the ability to tune the size of hollow silica spheres synthesized using catanionic vesicles as tempates.[56]

Conclusions

Inspired by recent findings that subcritical CO_2 can be employed to stabilize catanionic vesicles, we have developed a new method for vesicle-templated radical crosslinking photopolymerization for synthesis of hollow polymeric nanoparticles. Near equimolar aqueous solutions of SDS and DTAB precipitate immediately on mixing of the respective surfactant solutions, but remain stable for prolonged times under subcritical CO_2 (5 MPa). The vesicle bilayers

were swollen with the hydrophobic monomers *n*-butyl methacrylate/*tert*-butyl methacrylate/ethylene glycol dimethacrylate using diffusion loading, followed by UV-initiated radical crosslinking polymerization. This approach afforded polymeric nanocapsules in the approximate diameter range 40-100 nm (TEM/SEM), with their hollow structure confirmed by successful encapsulation and retention of Nile Blue dye. Using this CO2-based approach in conjunction with diffusion loading of monomers, it has been demonstrated that nanocapsules can be successfully prepared with monomer contents up to 94 wt% monomer relative to surfactant, which is comparable to the higher levels of monomer loading typically only achievable with concurrent loading protocols.[52-54]

The approach presented offers a novel route to polymeric nanocapsules of well-defined structure based on an environmentally friendly approach involving CO_2, thereby expanding the scope of available techniques for synthesis of such nano-objects with potential applications in a wide range of fields including nanomedicine (drug delivery), coatings and cosmetics applications.

Acknowledgements: P.B.Z. is grateful for a Future Fellowship from the Australian Research Council.

References

1. P. B. Zetterlund, Y. Kagawa and M. Okubo, *Chem. Rev.*, 2008, **108**, 3747-3794.
2. N. Konishi, T. Fujibayashi, T. Tanaka, H. Minami and M. Okubo, *Polym. J.*, 2010, **42**, 66-71.
3. T. Tanaka, Y. Komatsu, T. Fujibayashi, H. Minami and M. Okubo, *Langmuir*, 2010, **26**, 3848-3853.
4. S. Dong, W. Zhao, F. P. Lucien, S. Perrier and P. B. Zetterlund, *Polym. Chem.*, 2015, **6**, 2249-2254.
5. J.-T. Sun, C.-Y. Hong and C.-Y. Pan, *Polym. Chem.*, 2013, **4**, 873-881.
6. N. J. Warren and S. P. Armes, *J. Am. Chem. Soc.*, 2014, **136**, 10174-10185.
7. R. H. Utama, M. H. Stenzel and P. B. Zetterlund, *Macromolecules*, 2013, **46**, 2118-2127.
8. Y. Yan, M. Bjonmalm and F. Caruso, *Chem. Mater.*, 2014, **26**, 452-460.
9. H. Minami, H. Kobayashi and M. Okubo, *Langmuir*, 2005, **21**, 5655-5658.
10. P. B. Zetterlund, Y. Saka and M. Okubo, *Macromol. Chem. Phys.*, 2009, **210**, 140-149.
11. W. Meier, *Chem. Soc. Rev.*, 2000, **29**, 295-303.
12. C. J. McDonald and M. J. Devon, *Adv. Colloid Interface Sci.*, 2002, **99**, 181-213.
13. R. H. Utama, M. Drechsler, S. Foerster, P. B. Zetterlund and M. H. Stenzel, *ACS Macro Letters*, 2014, **3**, 935-939.
14. S. R. S. Ting, A. M. Gregory and M. H. Stenzel, *Biomacromolecules*, 2009, **10**, 342-352.
15. E. Amstad and E. Reimhult, *Nanomedicine*, 2012, **7**, 145-164.
16. Y. Luo and H. Gu, *Macromol. Rapid Commun.*, 2006, **27**, 21-25.
17. M. Okubo and H. Minami, *Colloid Polym. Sci.*, 1997, **275**, 992-997.
18. K. Landfester, *Ang. Chem. Int. Ed.*, 2009, **48**, 4488-4507.
19. E. T. A. van den Dungen and B. Klumperman, *J. Polym. Sci. Pol. Chem.*, 2010, **48**, 5215-5230.
20. E. Donath, G. B. Sukhorukov, F. Caruso, S. A. Davis and H. Mohwald, *Angew. Chem.-Int. Edit.*, 1998, **37**, 2202-2205.
21. Y. Wang, A. S. Angelatos and F. Caruso, *Chem. Mat.*, 2008, **20**, 848-858.
22. T. Addison, O. J. Cayre, S. Biggs, S. P. Armes and D. York, *Langmuir*, 2010, **26**, 6281-6286.
23. R. H. Utama, Y. Guo, P. B. Zetterlund and M. H. Stenzel, *Chem. Commun.*, 2012, **48**, 11103-11105.
24. S. Segota and D. Tezak, *Adv. Colloid Interface Sci.*, 2006, **121**, 51-75.
25. F. E. Antunes, E. F. Marques, M. G. Miguel and B. Lindman, *Adv. Colloid Interface Sci.*, 2009, **147**, 18-35.

26. T. Bramer, N. Dew and K. Edsman, *J. Pharm. Pharmacol.*, 2007, **59**, 1319-1334.
27. T. F. Tadros, *Int. J. Cosm. Sci.*, 1992, **14**, 93-111.
28. S. Gouin, *Trends in food science & technology*, 2004, **15**, 330-347.
29. P.-Y. Bolinger, D. Stamou and H. Vogel, *J. Am. Chem. Soc.*, 2004, **126**, 8594-8595.
30. E. Kaler, A. Murthy, B. Rodriguez and J. Zasadzinski, *Science*, 1989, **245**, 1371-1374.
31. E. W. Kaler, K. L. Herrington, A. K. Murthy and J. A. N. Zasadzinski, *J. Phys. Chem.*, 1992, **96**, 6698-6707.
32. C. Tondre and C. Caillet, *Adv. Colloid Interface Sci.*, 2001, **93**, 115-134.
33. J. N. Israelachvili, D. J. Mitchell and B. W. Ninham, *J. Chem. Soc.-Faraday Trans.*, 1976, **72**, 1525-1568.
34. A. Shioi and T. A. Hatton, *Langmuir*, 2002, **18**, 7341-7348.
35. S. A. Dergunov, S. C. Schaub, A. Richter and E. Pinkhassik, *Langmuir*, 2010, **26**, 6276-6280.
36. J. Hotz and W. Meier, *Langmuir*, 1998, **14**, 1031-1036.
37. S. Y. Liu, Y. I. Gonzalez and E. W. Kaler, *Langmuir*, 2003, **19**, 10732-10738.
38. J. Gomes, A. F. P. Sonnen, A. Kronenberger, J. Fritz, M. A. N. Coelho, D. Fournier, C. Fournier-Noel, M. Mauzac and M. Winterhalter, *Langmuir*, 2006, **22**, 7755-7759.
39. S. N. Shmakov and E. Pinkhassik, *Chem. Commun.*, 2010, **46**, 7346-7348.
40. M. Jung, I. den Ouden, A. Montoya-Goñi, D. H. W. Hubert, P. M. Frederik, A. M. van Herk and A. L. German, *Langmuir*, 2000, **16**, 4185-4195.
41. N. Poulain, E. Nakache, A. Pina and G. Levesque, *J. Polym. Sci. Pol. Chem.*, 1996, **34**, 729-737.
42. Z. Zhu, H. Xu, H. Liu, Y. I. Gonzalez, E. W. Kaler and S. Liu, *J. Phys. Chem. B*, 2006, **110**, 16309-16317.
43. C. McKelvey, E. Kaler, J. Zasadzinski, B. Coldren and H.-T. Jung, *Langmuir*, 2000, **16**, 8285-8290.
44. J. D. Morgan, C. A. Johnson and E. W. Kaler, *Langmuir*, 1997, **13**, 6447-6451.
45. D. H. Hubert, M. Jung and A. L. German, *Adv. Mater.*, 2000, **12**, 1291-1294.
46. S. A. Dergunov, K. Kesterson, W. Li, Z. Wang and E. Pinkhassik, *Macromolecules*, 2010, **43**, 7785-7792.
47. S. A. Dergunov, B. Miksa, B. Ganus, E. Lindner and E. Pinkhassik, *Chem. Commun.*, 2010, **46**, 1485-1487.
48. S. A. Dergunov and E. Pinkhassik, *Angew. Chem. Int. Ed.*, 2008, **47**, 8264-8267.
49. S. A. Dergunov, J. Durbin, S. Pattanaik and E. Pinkhassik, *J. Am. Chem. Soc.*, 2014, **136**, 2212-2215.

50. M. Jung, D. Hubert, P. Bomans, P. Frederik, J. Meuldijk, A. Van Herk, H. Fischer and A. German, *Langmuir*, 1997, **13**, 6877-6880.
51. M. Jung, B. H. Robinson, D. C. Steytler, A. L. German and R. K. Heenan, *Langmuir*, 2002, **18**, 2873-2879.
52. S. A. Dergunov, A. G. Richter, M. D. Kim, S. V. Pingali, V. S. Urban and E. Pinkhassik, *Chem. Commun.*, 2013, **49**, 11026-11028.
53. M. D. Kim, S. A. Dergunov, A. G. Richter, J. Durbin, S. N. Shmakov, Y. Jia, S. Kenbeilova, Y. Orazbekuly, A. Kengpeiil and E. Lindner, *Langmuir*, 2014, **30**, 7061-7069.
54. M. D. Kim, S. A. Dergunov and E. Pinkhassik, *Langmuir*, 2015, **31**, 2561-2568.
55. J. Zhang and B. Han, *Acc. Chem. Res.*, 2013, **46**, 425-433.
56. W. Li, J. Zhang, S. Cheng, B. Han, C. Zhang, X. Feng and Y. Zhao, *Langmuir*, 2009, **25**, 196-202.
57. W. Li, J. Zhang, B. Han and Y. Zhao, *Rsc Advances*, 2011, **1**, 776-781.
58. W. Li, J. L. Zhang, Y. J. Zhao, M. Q. Hou, B. X. Han, C. L. Yu and J. P. Ye, *Chem.-Eur. J.*, 2010, **16**, 1296-1305.
59. D. Pu, F. P. Lucien and P. B. Zetterlund, *J. Polym. Sci.; Part A: Polym. Chem.*, 2011, **49**, 4307-4311.
60. K. L. Herrington, E. W. Kaler, D. D. Miller, J. A. Zasadzinski and S. Chiruvolu, *J, Phys. Chem.*, 1993, **97**, 13792-13802.
61. P. Jokela, B. Joensson and A. Khan, *J. Phys. Chem.*, 1987, **91**, 3291-3298.
62. S. Dong, F. P. Lucien and P. B. Zetterlund, unpublished work.
63. M. Bergström and J. S. Pedersen, *Langmuir*, 1998, **14**, 3754-3761.
64. L. T. Banner, D. C. Danila, K. Sharpe, M. Durkin, B. Clayton, B. Anderson, A. Richter and E. Pinkhassik, *Langmuir*, 2008, **24**, 11464-11473.

Table 1. Recipe for mixed surfactant solution with monomer.

Mixed surfactant solution	**Quantity**
SDS	0.05 g (0.174 mmol)
DTAB	0.05 g (0.162 mmol)
Water	10 g
Monomer mixture	40-100 μL (0.047-0.118 g, 47-118 wt% rel. surf.)

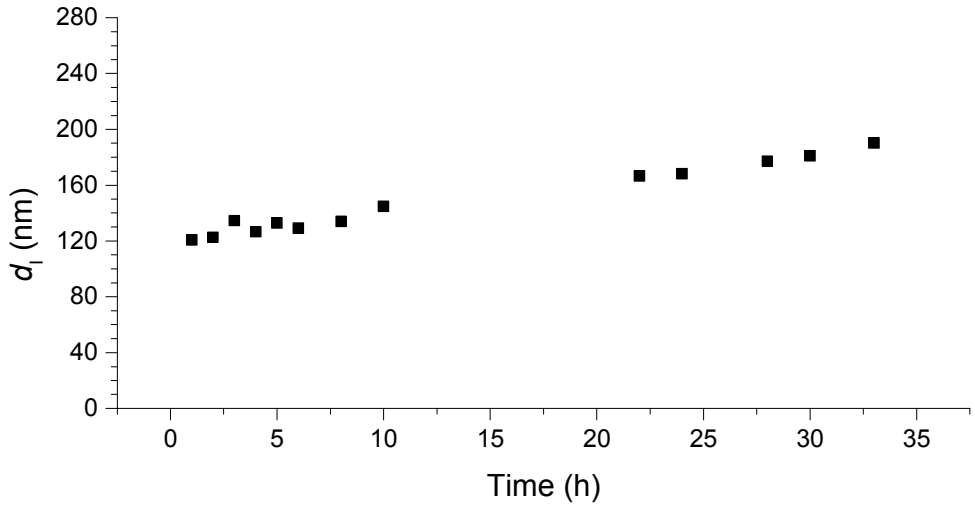

Fig. 1. Evolution of intensity-average diameter (d_I) over time for vesicle solution at 25 °C and a CO_2 pressure of 5.0 MPa before polymerization (recipe in Table 1; 47 wt% monomer (40 μL) rel. to total surfactant). See Fig. 3 for the corresponding size distributions.

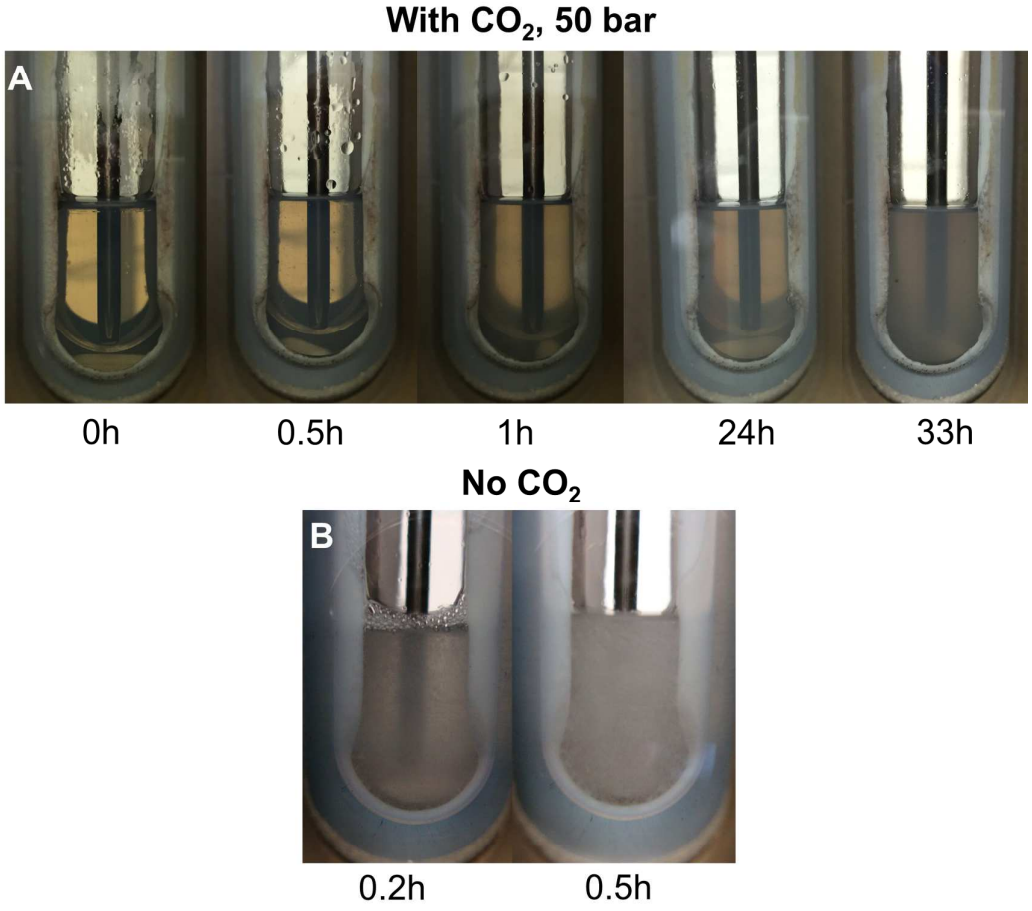

Fig. 2. Photographs of vesicle solution at 25 °C with (5.0 MPa) and without CO_2 before polymerization(recipe in Table 1; 47 wt% monomer (40 μL) rel. to total surfactant).

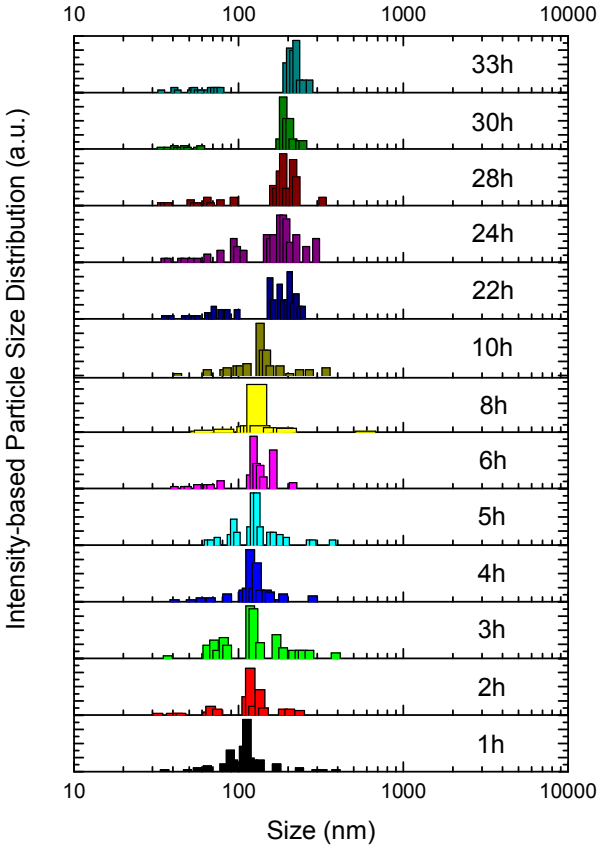

Fig. 3. Intensity-based size distributions for vesicle solution at 25 °C and a CO_2 pressure of 5.0 MPa before polymerization (recipe in Table 1; 47 wt% monomer (40 μL) rel. to total surfactant).

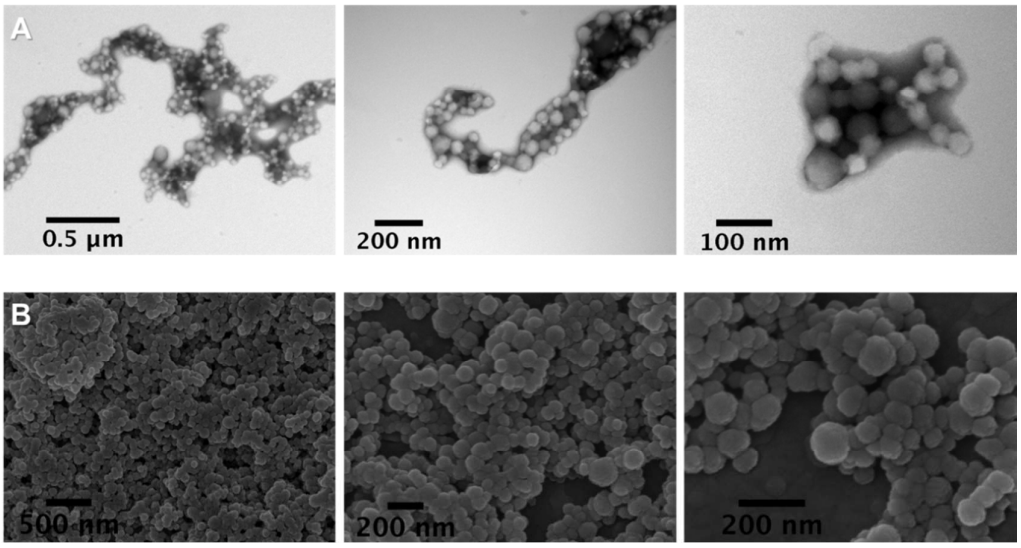

Fig. 4. TEM (A) and SEM (B) images of nanocapsules after polymerization and removal of surfactants for vesicle solution at 25 °C and a CO_2 pressure of 5.0 MPa (recipe in Table 1; 47 wt% monomer (40 µL) rel. to total surfactant).

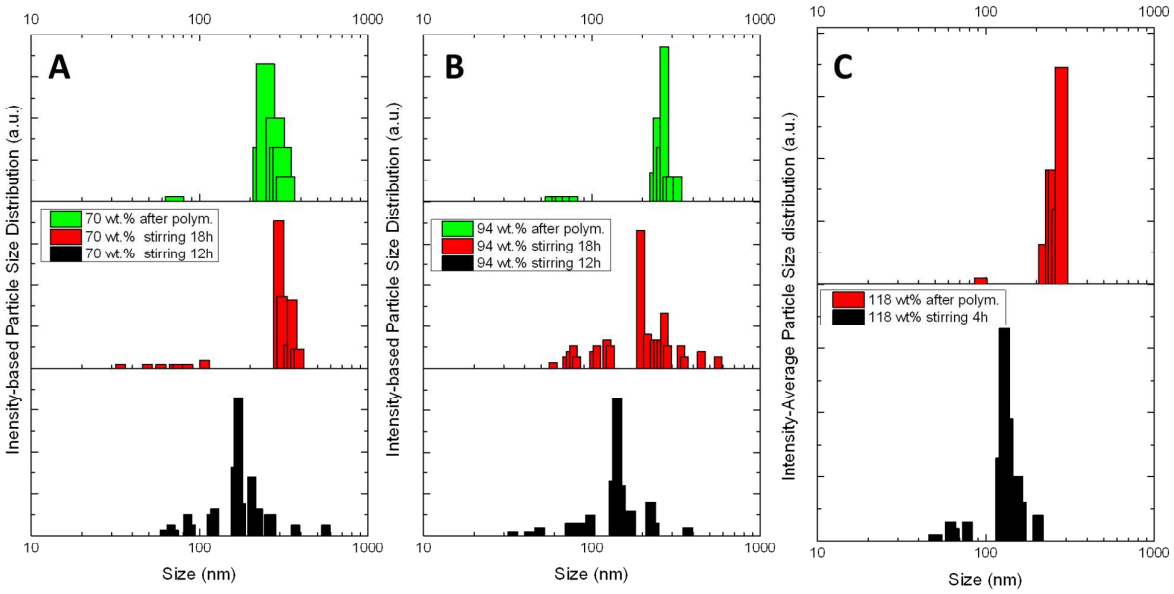

Fig. 5. Intensity-based size distribution for vesicle solution before and after polymerization at 25 ºC and a CO_2 pressure of 5.0 MPa for monomer loadings of 70 wt% (A), 94 wt% (B) and 118 wt% (C) (Table 1, wt% monomer rel. to total surfactant).

Table 2. Intensity-average diameters before and after polymerization at different monomer loadings.

Monomer loading (wt% rel. to total surfactant)	**Intensity-average diameter (number-average diameter) (nm)**	
	Before polymerization	After polymerization
70	303 (33)	267 (15)
94	210 (38)	254 (36)
118	131 (33)	259 (21)

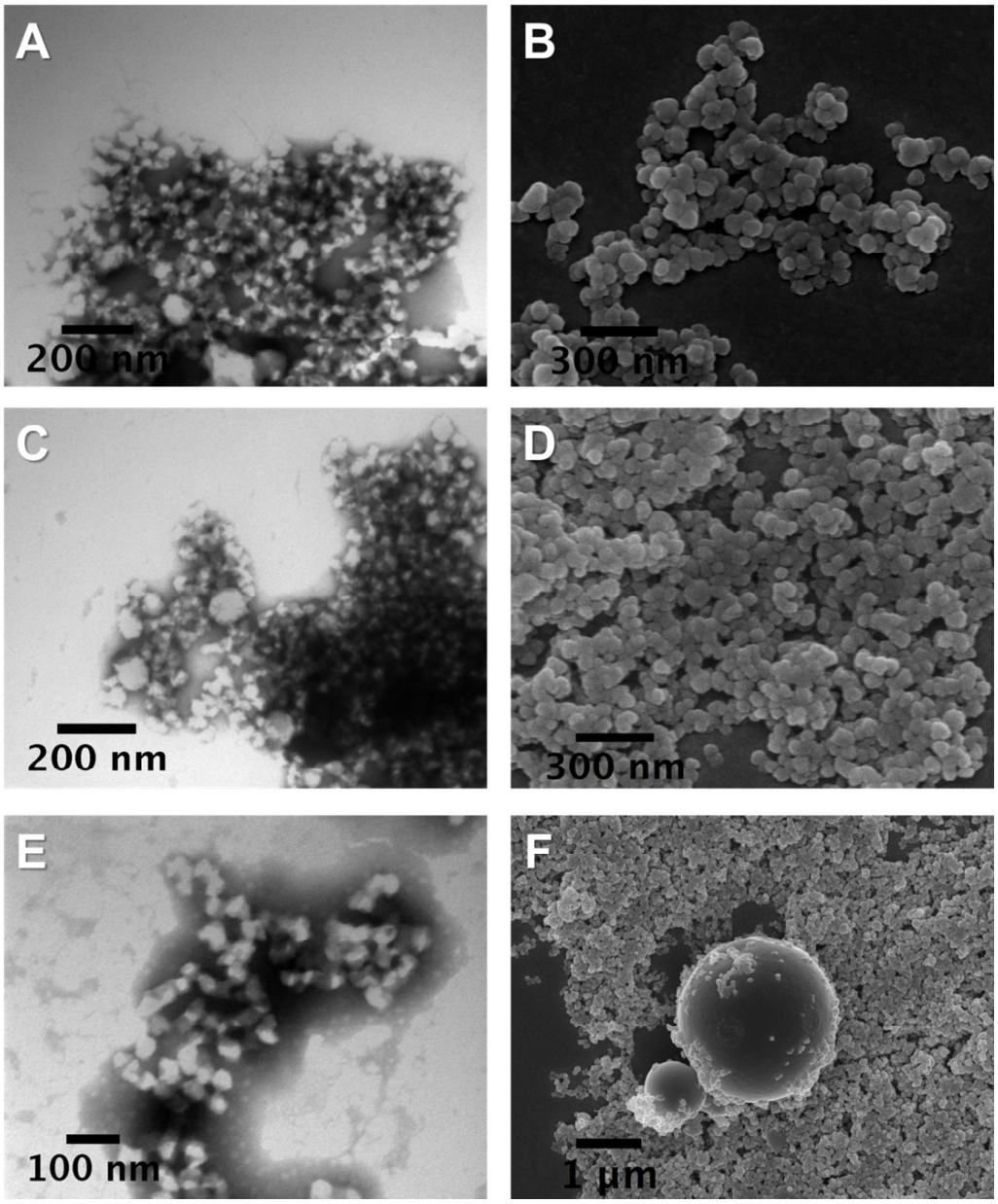

Fig. 6. TEM (A, C, E) and SEM (B, D, F) images of nanocapsules after polymerization and removal of surfactants for vesicle solution at 25 °C and a CO_2 pressure of 5.0 MPa (Table 1, monomer loading 70 wt% (A, B), 94 wt% (C, D), 118 wt% (E, F)).

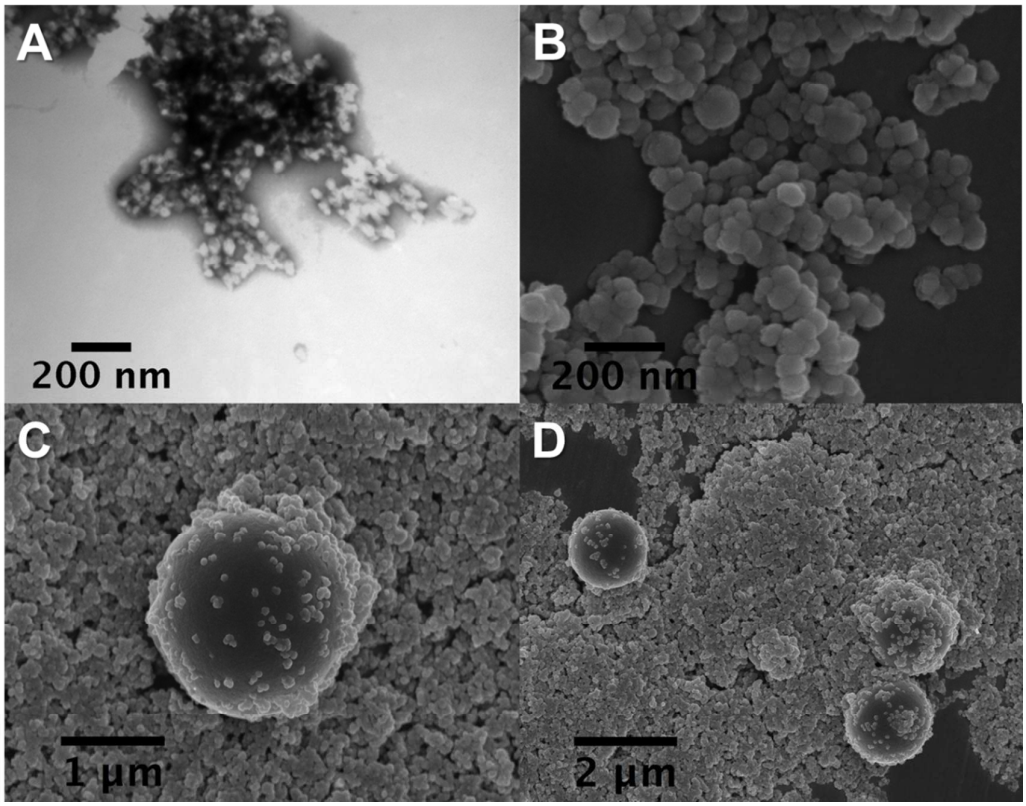

Fig. 7. TEM (A) and SEM (B, C, D) images of nanocapsules after polymerization and removal of surfactants for vesicle solution at 25 °C and a CO_2 pressure of 3.5 MPa (Table 1, 47 wt% monomer rel. to total surfactant).

Table of Contents Graphic

Synthesis of Crosslinked Polymeric Nanocapsules using Catanionic Vesicle Templates Stabilized by Compressed CO_2

Siming Dong, Patrick T. Spicer, Frank P. Lucien, Per B. Zetterlund*